Al-Jawoosh, S., Ireland, A., & Su, B. (2018). Fabrication and characterisation of a novel biomimetic anisotropic ceramic/polymer-infiltrated composite material. *Dental Materials*, *34*(7), 994-1002. https://doi.org/10.1016/j.dental.2018.03.008

Peer reviewed version

Fabrication and characterisation of a novel biomimetic anisotropic ceramic/polymer-infiltrated composite material

Abstract

Objective. To fabricate and characterise a novel biomimetic composite material consisting of aligned porous ceramic preforms infiltrated with polymer.

Method. Freeze-casting was used to fabricate and control the microstructure and porosity of ceramic preforms which were subsequently infiltrated with 40-50% by volume UDMA-TEGDMA polymer. The composite materials were then subjected to characterisation, namely density, compression, three-point bend, hardness and fracture toughness testing. Samples were also subjected to scanning electron microscopy and computerized tomography (Micro-CT).

Results. Three-dimensional aligned honeycomb-like ceramic structure were produced and full interpenetration of the polymer phase was observed using micro-CT. Depending on the volume fraction of the ceramic preform, the density of the final composite ranged from 2.92 to 3.36 g/cm^3, compressive strength ranged from 206.26 to 253.97 MPa, flexural strength from 97.73 to 145.65 MPa, hardness ranged from 1.46 to 1.62 GPa, fracture toughness from 3.91 to 4.86 MPa $m^{½}$. SEM observations of the fractured samples showed that crack propagation followed a tortuous path deflected by the polymer phase.

Significance. Freeze-casting provides a novel method to engineer composite materials with a unique aligned honeycomb-like interpenetrating structure, consisting of two continuous phases, inorganic and organic. There was a correlation between the ceramic fraction and the

Abbreviations: SEM, scanning electron microscopy; hrs, hours; UDMA, Urethane dimethacrylate; TEGDMA, Triethylene glycol dimethacrylate; vol., Volume; wt., weight; g, Gram; mm, Millimetre; µm, Micrometre; °C, Cellulose degrees; MCT, Micro Computerized Tomography; GPa, Gigapascal; MPa, Megapascal; N, Number; SD, Standard Deviation.

subsequent, density, strength, hardness and fracture toughness of the composite material.

Keywords:

Biomimetic composite; Porous ceramic; Microstructure; Gelatine; Polymer; Freeze casting;

Orthodontic brackets; Vickers Hardness; Strength; Fracture toughness.

Abbreviations: SEM, scanning electron microscopy; hrs, hours; UDMA, Urethane dimethacrylate; TEGDMA, Triethylene glycol dimethacrylate; vol., Volume; wt., weight; g, Gram; mm, Millimetre; µm, Micrometre; °C, Cellulose degrees; MCT, Micro Computerized Tomography; GPa, Gigapascal; MPa, Megapascal; N, Number; SD, Standard Deviation.

1 Introduction

Within both restorative dentistry and orthodontics there is a need for biomimetic materials that more closely approach the properties on natural tooth tissue. In restorative dentistry such a material could be used to restore tooth tissue lost through trauma or caries and such a hybrid dental ceramic is commercially available [1, 2] and is used with CAD/ CAM technology to mill dental restorations. In orthodontics such a material might be more aesthetic and have improved mechanical properties when compared with current aesthetic bracket materials. Orthodontic brackets are used to transmit loads from the archwire to the tooth[3], are most commonly metallic and bonded to the labial surfaces of the teeth which make them highly visible.

In the United States, from 1981 to 2013, the number of adults seeking orthodontic treatment grew from 15% to 23% [4] and as a result there have been increasing demands for more aesthetic, non-metallic bracket materials. Bracket material properties are influential in modulating the performance of the bracket during a course of orthodontic treatment and govern the bracket's ability to retain its structural integrity throughout the average 2 year course of treatment [5]. Currently available aesthetic orthodontic brackets are either made from a polymer e.g. polycarbonate or polyurethane, or a ceramic, usually alumina, either mono or polycrystalline in structure [6, 7].

Polymeric brackets, although aesthetically good at the start of treatment, are not popular due to: poor dimensional stability under applied load (creep), staining and low wear resistance [3, 6]. Although ceramic brackets do not suffer from these same disadvantages, they have their unique disadvantages, namely: brittleness with a tendency to fracture in-service, a high surface

hardness which can lead to abrasion of opposing teeth, and perhaps most importantly, an increased risk of enamel fracture during bracket removal [8, 9].

An ideal aesthetic orthodontic bracket would combine some of the advantages and none of the disadvantages of currently available polymeric and ceramic brackets. These would include improved wear resistance whilst minimising damage to opposing teeth, good stain resistance, good dimensional stability with minimal creep and ease of removal from the tooth surface at completion of treatment. Although two material phase brackets have been produced in the past, they have comprised principally a ceramic bracket with a thin polymeric bonding base. However, not only did these brackets possess many of the unwanted properties of ceramic brackets, namely brittleness and wear of opposing teeth, but the polymeric base would infrequently delaminate during service with subsequent loss of tooth control and requiring a new bracket to be used [10, 11].

Consequently, the development of a composite material that exhibits the advantages of both polymeric and ceramic brackets in a single interconnected network is therefore desirable. Certain naturally occurring biomaterials, including enamel and dentine, exhibit an interconnected dual phase structure leading to enhanced mechanical properties, which enable them to meet the biological functional needs of the organism [12]. Dental enamel is the hardest, most mineralised structure in the human body. It is composed of 96% to 97% hydroxyapatite, 1% collagen and 2% to 3% water. Throughout a lifetime, enamel can endure the forces of mastication over millions of cycles [13, 14]. By contrast, dentine is a porous mineralised structure that is composed of 70% hydroxyapatite, 20% collagen and 10% water by weight [15]. The aim of the present study is to produce a novel biomimetic ceramic/polymer

composite material for use as a possible orthodontic bracket material. The novelty of such a material would be defined by its unique microstructure, characterised by two continuous interconnected inorganic and organic phases as shown in Figure 1. With a polymer rich surface that can be attached to the tooth surface to aid bonding and debonding, and a ceramic rich surface directly exposed to the oral environment. In this way the final composite material will ideally combine the desirable properties of both ceramics and polymers, creating a durable, safe and aesthetically pleasing orthodontic bracket.

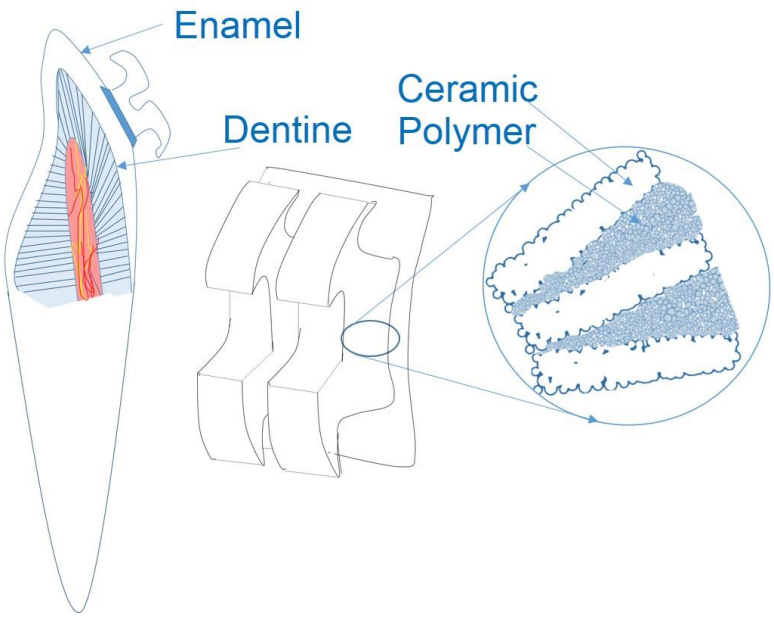

Figure 1. Schematic of the structure of the central incisor with the anisotropic feature of the biomimetic composite orthodontic bracket.

Freeze-casting is a well-established technique that can be used to fabricate porous scaffolds with complex microstructures. The process utilises the directional solidification of a ceramic suspension in a double-sided cooling/freezing device. The suspension is placed in a mould between two cooled surfaces, one of which is colder than the other and from where ice crystals

begin to form in a unidirectional fashion. As the suspension continues to freeze the ice crystals grow from the coldest to the less cold surface. In doing so they compress the ceramic particles to form an interconnected scaffold, which is then freeze dried and sintered. The technique is relatively simple, cost efficient, environmentally friendly and offers the ability to produce a porous material with a controlled-size and interconnection of the pores. A large number of processing parameters are used to tailor the final architecture of the porous scaffold, by controlling the crystal growth of ice [16, 17].

The principal aim of this study was to produce ceramic/polymer-infiltrated composite material through the mechanism of freeze-casting, to produce a porous alumina scaffold, followed by infiltration with UDMA-TEGDMA polymer. The effect of ceramic suspension concentration used for the freeze casting phase on the mechanical properties of the final ceramic polymer composite were also investigated.

2 Materials and methods

In this study, two novel expermental biomemetic ceramic/polymer composites were investigated, EBCI= experimental biomemetic composite with 30 vol.% ceramic in the aqueous suspension and EBCII= experimental biomemetic composite with 35 vol.% ceramic in the aqueous suspension.

2.1 suspension preparation

Alumina powder (CT3000, Almatis AC, Inc. Germany) with an average particle size of 0.6 µm was mixed with 0.6 wt% dispersant (Dolapix CE 64, Zschimmer & Schwarz GmbH, Germany) and dissolved in distilled water. Aqueous suspensions containing 30 and 35 vol.% ceramic concentrations were prepared in this study. Slurries were ball-milled in polyethylene bottles

using zirconia media in a ball-milling machine (SRT6, Stuart, UK) overnight in order to break down the agglomeration and achieve a more homogenous dispersion.

2.2 Gelatine concentration

In this study, gelatine powder (Type A, G250, Sigma Aldrich, UK) was used as a binder to increase the strength of the green ceramic scaffold. In order to study the effect of the gelatine on the structure of the final porous ceramic scaffold, ceramic aqueous suspensions containing 10 vol.% ceramic were prepared with gelatine added at a ratio of 2.5, 3.75, 5, 7.5 and 10 wt.% with respect to the ceramic powder dry weight. Gelatine powder was dissolved in distilled water, then the gelatine solution was added to the ceramic suspension in polyethylene bottle. The gelatine-alumina suspension was then ball-milled in a roller mixer machine (SRT6, Stuart, UK) in an oven (Thermo-Scientific, UK) heated to 55°C for 4 hrs.

2.3 Freeze-casting

The gelatine-alumina aqueous suspensions were poured into a custom-made non-porous cylindrical mould (diameter: 60 mm, height: 65 mm). Each suspension contained gelatine as a binder with 2.5% by weight in regard to the dry weight of the dry alumina powder in the suspension. The mould was made of a 20-mm thick acrylic ring, which acted to insulate the suspension, and a disc-shaped base made of copper, which was used as a freezing temperature carrier. The mould was then placed in a custom-built freeze-casting machine. The process for freeze-casting was carried out as previously described [18]. The temperatures were controlled through band heaters (MI, Watlow, USA) and thermocouples (Type J, Watlow, USA). The top rod was cooled using an immersion cooler (FT200, Julabo, Germany), while the bottom rod was

cooled using cooling apparatus (Polyscience, Illinois, USA). The bottom rod was cooled at a controlled rate of 1°C/min to -10°C whilst the temperature of the top rod was kept at 20°C. The sublimation of the ice took place in a vacuum in a Modulo Freeze Dryer (Edwards, Modulyo, UK) at −55 °C and 10^{-1} mbar for 48 hours. The green body was then carefully removed and sintered in a high-temperature furnace (Model BRF17/4M, Elite Thermal Systems Ltd., UK). The sintering occurred at a rate of 2°C/min up to a temperature of 400°C and maintained for 2 hours, followed by 10°C/min up to 1600°C and maintained for a further 2 hours. The samples were removed from the furnace after 24 hours to allow natural cooling.

2.4 Polymer infiltration

The sintered porous scaffolds were chemically treated with pre-hydrolysed 3-(trimethoxysilyl) propyl methacrylate coupling agent (Sigma- Aldrich, USA) to allow better bonding between the inorganic and organic phases. The porous ceramic scaffolds were infiltrated with a monomer mixture in a vacuum. The monomers were prepared by adding equal volumes of UDMA and TEGDMA and 1 vol.% of Luperox Benzoyl peroxide (Sigma-Aldrich, UK) as a heat activator. A self-contained vacuum impregnation system (Cast N'Vac Castable Vacuum System, Buehler, USA) was used to backfill the porous ceramic samples at a vacuum pressure of $4x10^{-2}$ mbar. The monomer/ceramic samples were then carefully placed in an oven at 50°C for 2 hours then at 60°C for 3 hours then 70°C for 6 hours and finally at 90°C for 12 hours to allow the heat polymerization of the monomers.

2.5 Cutting procedures

An Accutom-50 (Struers, UK) precise cutting machine was used to prepare the samples using a diamond saw (Beuhler, USA), cutting them into various sizes dependant on the test to be performed. The second stage of sample preparation involved polishing using a grinding machine (Tegra Pol 15, Struers, UK) with different sequential silicon carbide papers and water cooling. The final step of sample preparation was sonication in an ultrasonic water bath (Grant Scientific, UK) to remove any debris and unwanted particles.

2.6 Ceramic fraction measurements

The ceramic fraction in the ceramic/polymer composite structures was determined by heating the ceramic/polymer composite samples to 600°C to ensure complete removal of the organic phase; then the amount of the inorganic residues was calculated. The measurememnts of the initial composite specimen weights were performed then after the composite samples were heated in a furnace (Elite thermal systems Ltd., UK) in order to burn off the organic phase. The specimens were allowed to cool down in the furnace for 24 hrs, then they were removed and weighed. The weight fraction was then calculated from the initial weight of the ceramic/polymer composite structures. The volume fraction could then be calculated depending on the specific density of the composite constituents (Alumina=3.96, Polymer=1.21 g/cm^3).

2.7 Densities

The densities of the composite specimens were obtained by the Archimedes' method according to ASTM standard, C373−16, USA [19]. Rectangular blocks (4x4x8 mm) were prepared with all

their sharp edges and corners removed before the start of any measurement. The densities were calculated according to the following formula:

$$Density = \frac{Dry\ weight \times (\rho_{water} - \rho_{air})}{Dry\ weight - Suspended\ weight},$$

Where ρ_{water} and ρ_{air} are the density of deionized water and air respectively.

2.8 Sample imaging

The samples were imaged using SEM (FEI Quanata 400, FEI, USA) after being coated with a gold palladium mixture (Emitech K575X, Quorum Technology Ltd, UK). Images of the samples were also produced using a Micro-CT scanner (Nikon XTH320 CT scanner, Japan), with isotropic voxels and a spatial resolution of 13 µm. These Micro-CT images were used to reconstruct three-dimensional models of the scaffolds. The three-dimensional reconstruction of the model of each scaffold was performed from the stacking of the two-dimensional images using specialized software (Simpleware, UK).

2.9 Compressive strength

Five rectangular specimens (4 x 4 x8 mm) of each ceramic/polymer composite material were tested using a universal testing machine (Zwick Roell Z020, Ulm, Germany). The compressive force was directed along the long axis of the specimens and in the same direction as the freeze-casting, with the polymer rich surface at the top and the ceramic rich surface at the bottom. The compressive strength σ_C was calculated according to the following formula, where *F* is the load at fracture and *A* is the cross-sectional area:

$$\sigma c = \frac{F}{A}$$

2.10 Flexural strength and elastic modulus

Three-point bending was used to determine the flexural strength of the composite samples in this study. Samples (1.8x4x18 mm) were loaded into a computer-controlled universal machine according to British Standard, BS EN ISO 6872, 2008 [20]. For this test, the samples were divided into two different groups; one group was tested with the force directed parallel to the direction of freeze-casting and the other with the force applied perpendicular to the direction of freeze-casting. After the force was loaded and the maximum load was reached, all the samples were removed and checked to make sure that the fracture point was at the centre. Flexural strength, σ_f, was calculated according to the formula:

$$\sigma f = \frac{3FL}{2WH^2}$$

Where *F* is the load at fracture, *L* the span length, *W* the specimen width and *H* the specimen height.

The elastic modulus was determined from the three-point bending results and calculated on formula:

$$E = \frac{F * l^3}{4 * D * W * H^3}$$

where D is the deflection corresponding to load.

2.11 Hardness

Surface hardness was measured using a micro-based indentation system (Duramin Ver 0.08, Struers, UK) under a load of 9.807 Newton with a calibrated Vickers indenter according to the Standards of Advanced Technical Ceramics, EN843-4: 2005[21]. Six rectangular specimens (4x10x12 mm) were subjected to a maximum load for 20 seconds and 30 determinations were made for each material. Indentation diagonals were measured by light microscopy. Any indentations with an irregular shape were rejected.

2.12 Fracture toughness

Six rectangular specimens of each composite sample (32x8x4 mm) were polished and pre-notched with a high-speed cutting machine according to the Standards for a single-edge-notched beam, ASTM 1820.15.A,USA [22]. Then, a razor blade and diamond paste were employed to sharpen the notch and extend it an additional 200–350.89µm. The final length of the notch was measured with an optical microscope. All the samples were loaded in a universal testing machine (Zwick Roell Z020, Ulm, Germany). The fracture toughness K_{1C} was calculated according to the formula:

$$K^{1}{}_{C}\frac{Fl}{BW^{\frac{3}{2}}}f\left(\frac{\dot{\alpha}}{w}\right)$$

F is the load at fracture, L is the span length, B is the breadth of the beam, W is the width of the beam, and a is the length of the notch. Geometrical factor *f (ȧ/w)* can be calculated by the following equation:

$$f(\frac{\dot{\alpha}}{w}) = 3(\frac{\dot{\alpha}}{w})^{1/2} x (1.99 - (\frac{\dot{\alpha}}{w}) x \left(1 - (\frac{\dot{\alpha}}{w})\right) x 2.15 - 3.93(\frac{\dot{\alpha}}{w}) + 2.7(\frac{\dot{\alpha}}{w})^2))/2(1 + 2(\frac{\dot{\alpha}}{w})) x (1 - (\frac{\dot{\alpha}}{w}))^{3/2}$$

2.13 Statistical Analysis

The data were analysed using Stata version 14 (Stata Corp, College Station, Texas, USA) with a predetermined significance level of alpha = 0.05. Summary statistics are illustrated in Table 1 along with the means and 95% confidence intervals of the means and the results of the Shapiro-Wilks test. The data were found to be normally distributed in the majority of cases. Therefore t-tests were used for direct comparison between pairs of tests for the two materials EBCI and EBCII.

3 Results

The principle aim of this study was to fabricate a biomimetic composite material with fully interconnected networks of ceramic and polymer and with an intimate ceramic/polymer interface. Two different ceramic concentrations were prepared in the aqueous ceramic suspensions (30 and 35 vol.%) with gelatine concertation 2.5% by weight in regard to the dry weight of alumina powder. The slurries then were freeze-cast followed by sublimation and sintering. The use of gelatine as a binder in combination with freeze casting techniques allowed tuneable formation of three-dimensional structures with pores in the micrometre range and a honeycomb-like shape. Honeycomb ceramic scaffolds were produced as illustrated in Figure 2.

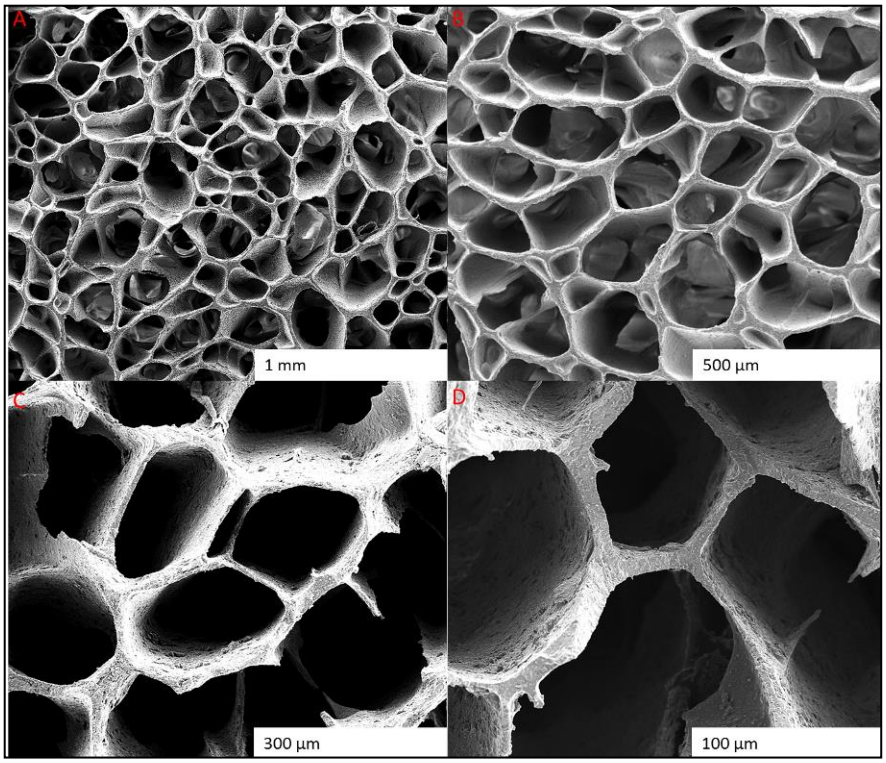

Figure 2. SEM images showing honey-comb cross-section of the porous ceramic scaffold with different magnifications in cross section perpendicular to the freezing direction. (A x50, B x75, C x180 and D x300).

Firstly, the effect of gelatine concentration on the microstructure of ceramic scaffold was investigated. As the initial gelatine concentrations increased the pores became more rounded and some hexagonal in shape. Not only did the ceramic wall thickness decrease with increasing gelatine concentration, but so did the size of the pores (Figure 3).

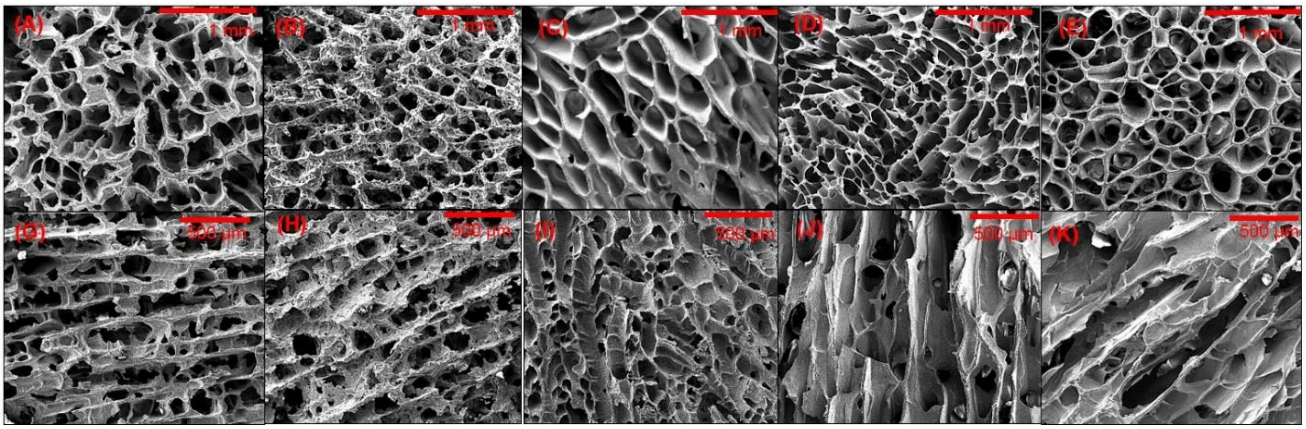

Figure 3. SEM images showing the microstructure of six different ceramic samples with different gelatine concentrations: 2.5% (*A x50, G x75*), 3.75% (*B x50, H x75*), 5% (*C x50, I x70*), 7.5% (*D x50, J x70*) and 10% (*E x50, K x75*). The plane of the cross-sectional images is perpendicular and parallel to the freezing direction respectively.

3.1 Densities

As the initial ceramic suspension concentration increased from 30 to 35 vol.% the ceramic volume of the final composite was observed to rise from 50.89% (EBCI) to 61.17% (EBCII). By increasing the ceramic volume fraction of the composite by 10%, the densities increased from a mean value of 2.9 to 3.4 g/cm^3, although when considering the 95% confidence intervals there was little difference. Micro-CT confirmed this trend, with the % volumes being 51.27% and 62.91% respectively.

3.2 Sample imaging

Micro-CT examination revealed the structure of the composite material as a fully interconnected network of a polymeric phase within a ceramic network phase. Three-dimensional reconstruction of the ceramic and polymer networks showed almost a complete infiltration of the polymer phase in the ceramic porous preform (Figure 4).

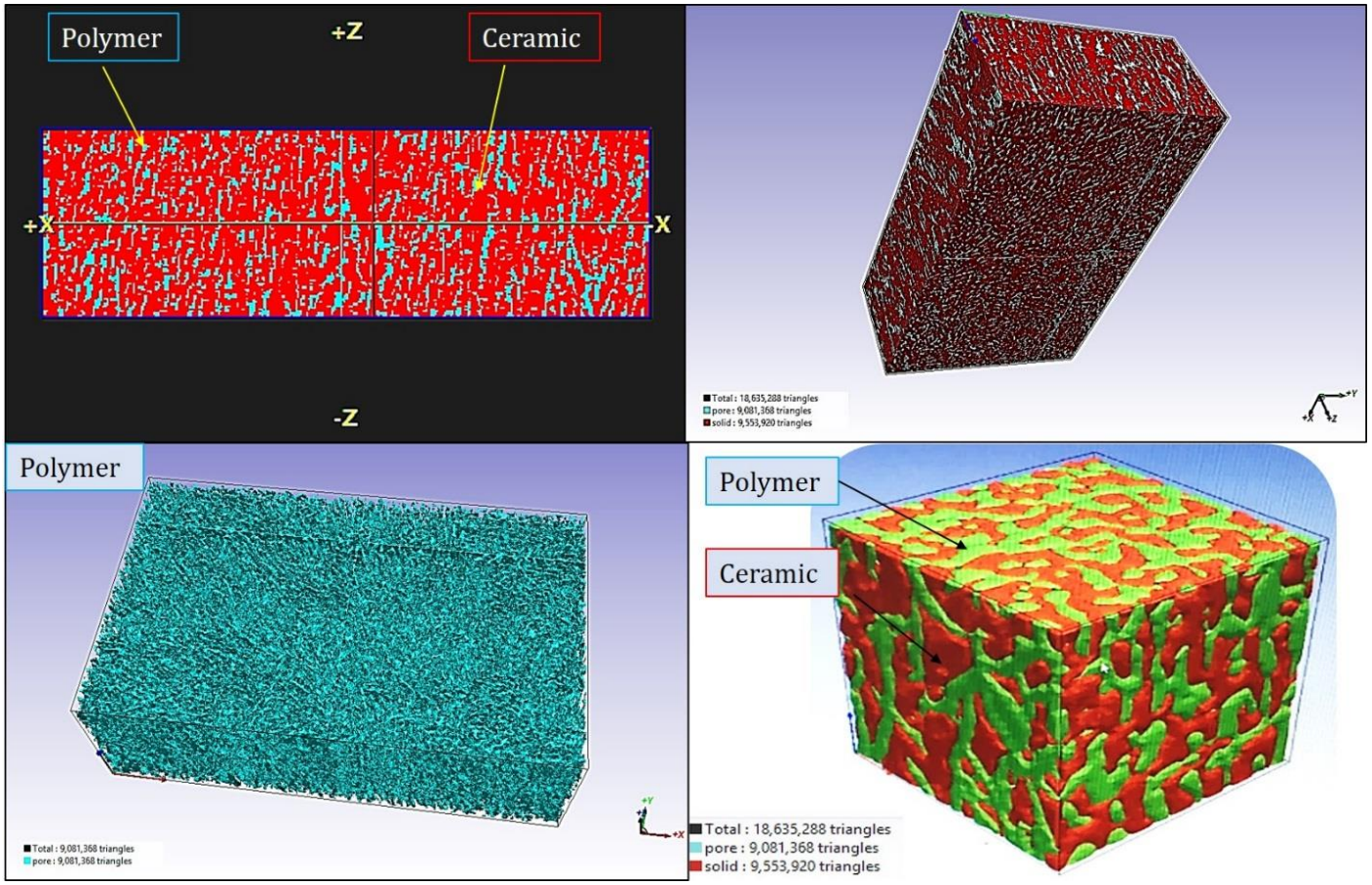

Figure 4. Micro-CT images representing the final composite material. Different colours represent different substances; red represents the ceramic phase, green represents the polymer phase and black represents air (less than 2%).

Table 1. Summary data tables for EBCI and EBCII including means, SD, 95% confidence intervals of the means and Shapiro-Wilk test (Prob>z) for normality.

Variable	EBCI					EBCII				
	N	Mean	SD	[95% Conf. Interval]	Prob>z	N	Mean	SD	[95% Conf. Interval]	Prob>z
Density (g/cm^3)	5	2.92	0.33	2.52 to 3.33	0.47	5	3.36	0.32	2.96 to 3.76	0.58
Compressive strength (MPa)	5	253.97	19.23	230.06 to 277.84	0.35	5	206.26	20.29	181.06 to 231.46	0.89
Flexural strength parallel to freezing direction (MPa)	30	97.73	21.12	89.84 to 105.61	0.08	21	145.65	32.50	128.62 to 162.68	0.10
Flexural strength perpendicular to freezing direction (MPa)	6	111.57	7.36	103.84 to 119.30	0.59	6	129.18	13.96	114.52 to 143.83	0.50
Fracture toughness (MPa $m^{½}$)	6	4.86	1.03	3.77 to 5.94	0.17	6	3.91	0.42	3.47 to 4.34	0.23
Hardness (GPa)	6	1.46	0.11	1.35 to 1.58	0.06	6	1.62	0.09	1.51 to 1.71	0.54
Modulus of elasticity (GPa)	15	15.53	4.37			12	16.56	3.92		

3.3 Compressive strength

Unlike density, the compressive strength of the novel biomimetic composite fell as the fraction volume of ceramic in the composite increased with the mean compressive strength for EBCII being 206.26 and for EBCI, the mean value was to 253.97 MPa. However, once again when considering the 95% confidence intervals the difference is unlikely to be significant.

3.4 Flexural strength

With increasing the volume fraction of ceramic in the composite material the flexural strength of the hybrid composite increased from 97.73 to 145.65 MPa parallel to the direction of freeze casting and from 111.57 to 129.18 MPa perpendicular to the direction of freeze casting.

3.5 Elastic modulus

The elastic modulus of each of the composite materials, EBCI and EBCII were similar at mean value of 15.53 and 16.56 GPa respectively.

3.6 Hardness

As the ceramic suspension concentration increased there was again little change in the observed mean hardness values, which were 1.46 GPa and 1.62 GPa for the EBCI and EBCII.

3.7 Fracture Toughness

There was a trend for a small reduction in observed mean fracture toughness 4.86 and 3.91 GPa as the ceramic volume fraction increased for EBCI and EBCII.

4 Discussion

The main aim of this research was to develop a new composite material which is composed of ceramic and polymer networks using a novel fabrication method. Rather than one continuous

organic polymer phase filled with inorganic particles in the conventional dental composite, the new composite material possesses co-continuous interpenetrating phases of ceramic and polymer with anisotropic microstructure, which potentially can overcome many withdraw backs oy pure ceramics or polymers for aesthetic orthodontic applicants.

It is anticipated that such a new composite material could provide good bonding and debonding properties to the teeth via the organic phase and good wear resistance to brushing via the inorganic phase.

Freeze casting is a technique that can form porous ceramic scaffold by means of solidification of a ceramic suspension by subjecting it to a temperature gradient followed by sublimation and sintering[23]. Alumina powder was used in the present study as it is the most popular ceramic material that has been used to fabricate orthodontic brackets due to its biocompatibility, high wear resistance, good aesthetic and high strength [24]. In this study, the porous ceramic scaffolds characterized by an anisotropic honeycomb-like porous micro-structure rather than lamellar pore structures typically seen for freeze cast scaffolds [25]. These results are in agreement with other studies on microporous ceramics with very high porosities and honey comb structure through the use of gelatine as a binder [20]. The characteristic honey-comb like structure is believed to be formed as the result of the gelatine gelation effect during the freezing process[26]. These structures mimic teeth as they resemble the honeycomb-like appearance in the dentin-enamel junction which characterise the distribution of the dental organic material in inorganic phase in teeth [27]. The SEM images reveals honey-comb-like cylindrical pores perpendicular to the freezing direction with various sizes are formed because

of the ceramic particles expelled by water molecules and packed between the growing ice crystals in the gelatine-based ceramic suspension [16, 26].

Gelatine is a biopolymer that is widely used in composite materials due to its non-toxicity, biological origin and good mechanical properties. It is denatured collagen which undergoes physical gelation at temperatures below 15-20 °C forming a weakly crosslinked network. It can produce distinctively tailored porous scaffold when combined with freeze casting. High porosities and high strength are two of the main advantages that have been found in porous structures produced by combining gelation and freeze casting [28, 29].

An increase in gelatine concentration resulted in more rounded honeycomb-like pores and a decrease in the dimensions of the ceramic walls. One possible explanation is that, with the increased concentration of gelatine, and the viscosity of ceramic suspension increased, and a higher force was needed for weakly cross-linked gelatine and ceramic molecules to be expelled by water molecules. The gelled suspension increased the movement resistance of water and ice crystals can no longer grow in their typical plate-like morphology and form lamellar structure in the ceramic suspension.

Composites with interpenetrating phase and honey-comb like microstructures can have good mechanical and tribological properties especially shear strength and wear when compared to those with lamellar structures [2, 29-32].

A previous study by Petrini etal [33] showed a biomimetic composite with mechanical properties similar to those of the dentin through the use of an epoxy polymer in a lamellar structured porous ceramic scaffold.

In the present study, UDMA polyacrylate polymer was used to explore the possibility of fabricating a biomimetic composite material that can be used in the oral cavity with desirable physical and mechanical properties due to its biocompatibility. Widely used as a dental polymer in composite formulations for restorative purposes and it has also been investigated for the use as an orthodontic bracket in the literature [34-36]. TEGDMA monomer was used as a low viscosity diluent agent for a better infiltration due to the high viscosity and multiple functional groups of UDMA [37].

The density and mechanical properties of the novel composite materials increased with the increase of ceramic volume fraction. This is in agreement with previous studies on hybrid composite dental materials [2, 38]. The compressive strength in this study ranged from 206.26 to 253.97 MPa which is higher than that of enamel 62-89 MPa and comparable to that of the dentine 194-224 MPa [39]. The flexural strength of the biomimetic ceramic/polymer composite was 97.73 and 145.65 MPa for EBCI and EBCII respectively. These data suggest that the greater the inorganic content in the novel composite material the higher its flexural strength, in agreement with previous studies on dental composite materials [40, 41]. Moreover, these values are higher than that found for feldspathic porcelain (65 MPa), enamel (60-90 MPa), slightly higher than the traditional dental composite (139 MPa) and lower when comparable to that of dentine (245-280) [42].

The flexural strength also showed anisotropy depending on whether the force was applied parallel or perpendicular to the freezing direction. A higher strength was observed when load applied perpendicularly. These results can be attributed to the arrangement of the ceramic

walls in the composite material and indicate the presence of anisotropic structure which resemble that of the enamel and dentine [43, 44].

From the three-point bending test, the elastic modulus was calculated, and it was in the range of 15.53 and 16.56 GPa. These values are higher than those obtained from the compressive strength testing of the enamel and dentine (1.34 and 1.65 GPa respectively).

Hardness is defined as the resistance to a permanent surface indentation and affects the material's wear resistance [45]. In this study, the hardness values of the composite material ranged between 1.4 and 1.6 GPa which is lower than that of enamel and other dental materials such as Enamic, Zirconia and Lithium Disilicate glass ceramics are 3.43, 3.31, 13.94 and 10 GPa respectively, suggesting the suitability of the material in relation to enamel for future use in the oral cavity[42]. Materials with a high hardness value might not be desirable for dental use since they may result in abrasion of the opposing teeth[46-50]. On the other hand, the novel composite material present low hardness when compared to stainless steel and Nickel-titanium archwire alloys. During orthodontic treatment this may induce higher rates of wear and insufficient slot-wire engagement [51].

Fracture toughness is the measure of the material's ability to absorb strain energy prior to fracture [52]. The average fracture resistance of tooth enamel and dentin are approximately 0.72 to 1.28 and 2.2 to 3.1 MPa $m^{½}$ respectively [49, 53, 54]. The mean values of the fracture toughness in this study were 3.91 MPa $m^{½}$ and 4.86 MPa $m^{½}$ for EBCII and EBCI.

Aesthetic orthodontic brackets are made either from ceramic or plastics which have the disadvantages of brittleness and low wear resistance respectively. The novel composite

material has an interpenetrating structure thus it can have the advantages of both organic and inorganic phases in an anisotropic character which may be desirable for the design and fabrication of orthodontic bracket material.

For the novel composite materials to be used as an orthodontic bracket, fabrication of a brackets is essential to determine their machinability and suitability. Further tests are required to clarify if the novel biomimetic composite material is applicable for potential orthodontic bracket use such as bonding and abrasive tests. Moreover, several implications related to wear resistance, water absorption, tie-wing strength, torque control future and simulation of clinical conditions are important. To date, there are no studies in literature on biomimetic composite material that mimic the architectural design of tooth structures and aimed for the use as orthodontic bracket material.

5 Conclusion

This study demonstrated that the freeze-casting technique can produce porous ceramic scaffolds with interconnected pores in a three-dimensional and honeycomb-like structure at various gelatine concentrations. The gelatine binder in the initial gelatine/alumina suspension had a significant effect on the microstructure of the porous ceramic scaffolds. It was possible to produce composite materials with two continuous ceramic and polymer phases and different ceramic volume fractions. Imaging characterization and analysis confirmed that the composite materials are different from the traditional composites and ceramics currently used in dentistry. It was shown that, by controlling the solid loading in the initial ceramic aqueous suspension, the physical and mechanical properties of the composite material can be tailored.

There is a correlation between the mechanical properties of the ceramic/polymer composite materials, their composition and their microstructure.

Acknowledgements

We sincerely thank the Higher committee of Education Development in Iraq, Baghdad, Iraq for providing the financial support, Dr. Steven Rae for his help in fracture toughness measurements (ACCIS, Department of Aerospace Engineering, University of Bristol, UK) and the Wolfson Bioimaging Facility (University of Bristol, UK) for their help in obtaining the SEM images.

References

[1] L.-H. He, M. Swain, A novel polymer infiltrated ceramic dental material, Dental Materials 27(6) (2011) 527-534.
[2] A. Coldea, M.V. Swain, N. Thiel, Mechanical properties of polymer-infiltrated-ceramic-network materials, Dental Materials 29(4) (2013) 419-426.
[3] W.R. Proffit, H.W. Fields, D.M. Sarver, Contemporary Orthodontics, 5th Edition, Mosby, Inc., an affiliate of Elisive Inc.2012.
[4] L. Christensen, F. Luther, Adults seeking orthodontic treatment: expectations, periodontal and TMD issues, British Dental Journal 218(3) (2015) 111-117.
[5] T. Eliades, N. Pandis, Self-Ligation in Orthodontics. An evidence-based approach to biomechanics and treatment, Blackwell Publishing Ltd2009.
[6] J.C. Feldner, N.K. Sarkar, J.J. Sheridan, D.M. Lancaster, IN-VITRO TORQUE-DEFORMATION CHARACTERISTICS OF ORTHODONTIC POLYCARBONATE BRACKETS, American Journal of Orthodontics and Dentofacial Orthopedics 106(3) (1994) 265-272.
[7] R.R. Kusy, Orthodontic biomaterials: From the past to the present, Angle Orthodontist 72(6) (2002) 501-512.
[8] V.A.J. Buzzitta, S.E. Hallgren, J.M. Powers, BOND STRENGTH OF ORTHODONTIC DIRECT-BONDING CEMENT-BRACKET SYSTEMS AS STUDIED INVITRO, American Journal of Orthodontics and Dentofacial Orthopedics 81(2) (1982) 87-92.
[9] J.B. Douglass, ENAMEL WEAR CAUSED BY CERAMIC BRACKETS, American Journal of Orthodontics and Dentofacial Orthopedics 95(2) (1989) 96-98.
[10] M.E. Olsen, S.E. Bishara, J.R. Jakobsen, Evaluation of the shear bond strength of different ceramic bracket base designs, Angle Orthodontist 67(3) (1997) 179-182.
[11] S. Elekdag-Turk, D. Isci, N. Ozkalayci, T. Turk, Debonding characteristics of a polymer mesh base ceramic bracket bonded with two different conditioning methods, European Journal of Orthodontics 31(1) (2009) 84-89.
[12] E. Munch, M.E. Launey, D.H. Alsem, E. Saiz, A.P. Tomsia, R.O. Ritchie, Tough, Bio-Inspired Hybrid Materials, Science 322(5907) (2008) 1516-1520.
[13] A. Nancy, Ten Cate's Oral Histology: Development,Structure,and Function, 7th. ed., Mosby Inc,Saint Louis2008.

[14] L.H. He, Z.H. Yin, L.J. van Vuuren, E.A. Carter, X.W. Liang, A natural functionally graded biocomposite coating - Human enamel, Acta Biomaterialia 9(5) (2013) 6330-6337.
[15] P. Zaslansky, S. Zabler, P. Fratzl, 3D variations in human crown dentin tubule orientation: A phase-contrast microtomography study, Dental Materials 26(1) (2010) E1-E10.
[16] S. Deville, Freeze-Casting of Porous Biomaterials: Structure, Properties and Opportunities, Materials 3(3) (2010) 1913-1927.
[17] Y. Zhang, K. Zuo, Y.-P. Zeng, Effects of gelatin addition on the microstructure of freeze-cast porous hydroxyapatite cerarmics, Ceramics International 35(6) (2009) 2151-2154.
[18] A. Preiss, B. Su, S. Collins, D. Simpson, Tailored graded pore structure in zirconia toughened alumina ceramics using double-side cooling freeze casting, Journal of the European Ceramic Society 32(8) (2012) 1575-1583.
[19] A. International, Standard Test Methods for Determination of Water Absorption and Associated Properties by Vacuum Method for Pressed Ceramic Tiles and Glass Tiles and Boil Method for Extruded Ceramic Tiles and Non-tile Fired Ceramic Whiteware Products1, C373 − 16´1, 2016.
[20] BSI, Dentistry. Ceramic materials, BSI, 2008.
[21] BSI, Advanced technical ceramics. Mechanical properties of monolithic ceramics at room temperature. Vickers, Knoop and Rockwell superficial hardness, BSI, 2007.
[22] A. Iternational, Standard Test Method for Measurement of Fracture Toughness1, American Society for Testing and Materials, 2011.
[23] S. Deville, Freeze-casting of porous ceramics: A review of current achievements and issues, Advanced Engineering Materials 10(3) (2008) 155-169.
[24] M.C.C.d.S.e.B.d.M.C.N.E.J.D.F.L.G.d. Oliveira, Mechanical Properties of Alumina-Zirconia Composites for Ceramic Abutments, Materials Research 4(4) (2004) 643-649.
[25] H. Park, M. Choi, H. Choe, D.C. Dunand, Microstructure and compressive behavior of ice-templated copper foams with directional, lamellar pores, Materials Science and Engineering a-Structural Materials Properties Microstructure and Processing 679 (2017) 435-445.
[26] M. Fukushima, M. Nakata, Y.-i. Yoshizawa, Fabrication and properties of ultra highly porous cordierite with oriented micrometer-sized cylindrical pores by gelation and freezing method, Journal of the Ceramic Society of Japan 116(1360) (2008) 1322-1325.
[27] N. Amizuka, T. Uchida, M. Fukae, M. Yamada, H. Ozawa, ULTRASTRUCTURAL AND IMMUNOCYTOCHEMICAL STUDIES OF ENAMEL TUFTS IN HUMAN PERMANENT TEETH, Archives of Histology and Cytology 55(2) (1992) 179-190.
[28] M.D.J.L.P. Papon, Gelation of aqueous gelatin solutions. I. Structural investigation, Journal de Physique 49(2) (1988) 319-32.
[29] M. Fukushima, Y. Yoshizawa, T. Ohji, Macroporous Ceramics by Gelation-Freezing Route Using Gelatin, Advanced Engineering Materials 16(6) (2014) 607-620.
[30] C.G. Long, Y. Su, C. Shen, Mechanical and Tribological Properties of Polytetrafluoroethylene filled Polyoxymethylene/Aluminum Foam Interpenetrating Phase Composites, in: Y.H. Kim, P. Yarlagadda (Eds.), Research in Materials and Manufacturing Technologies, Pts 1-32014, pp. 285-289.
[31] Q.C. Zhang, X.H. Yang, P. Li, G.Y. Huang, S.S. Feng, C. Shen, B. Han, X.H. Zhang, F. Jin, F. Xu, T.J. Lu, Bioinspired engineering of honeycomb structure - Using nature to inspire human innovation, Progress in Materials Science 74 (2015) 332-400.
[32] R. Lakes, MATERIALS WITH STRUCTURAL HIERARCHY, Nature 361(6412) (1993) 511-515.
[33] M. Petrini, M. Ferrante, B. Su, Fabrication and characterization of biomimetic ceramic/polymer composite materials for dental restoration, Dental Materials 29(4) (2013) 375-381.
[34] I. Sideridou, V. Tserki, G. Papanastasiou, Study of water sorption, solubility and modulus of elasticity of light-cured dimethacrylate-based dental resins, Biomaterials 24(4) (2003) 655-665.

[35] A. Faltermeier, M. Behr, D. Mossig, In vitro colour stability of aesthetic brackets, European Journal of Orthodontics 29(4) (2007) 354-358.
[36] J. Krauss, A. Faltermeier, M. Behr, P. Proff, Evaluation of alternative polymer bracket materials, American Journal of Orthodontics and Dentofacial Orthopedics 137(3) (2010) 362-367.
[37] C.J.E. Floyd, S.H. Dickens, Network structure of bis-GMA- and UDMA-based resin systems, Dental Materials 22(12) (2006) 1143-1149.
[38] L.-H. He, D. Purton, M. Swain, A novel polymer infiltrated ceramic for dental simulation, Journal of Materials Science-Materials in Medicine 22(7) (2011) 1639-1643.
[39] J.L. KJ Chun; HH Choi;, Comparison of mechanical property and role between enamel and dentin in the human teeth, Journal of Dental Biomechanics 5 (2014).
[40] I.W.F.M. Mueller, Effect of filler content of restorative resins on retentive strength to acid-conditioned enamel, Am J Dent. 7(3) (1994) 161-6.
[41] K.H. Kim, J.L. Ong, O. Okuno, The effect of filler loading and morphology on the mechanical properties of contemporary composites, Journal of Prosthetic Dentistry 87(6) (2002) 642-649.
[42] R.S.a.J. Powers, Craig's Restorative dental materials, 13 ed., Mosby St. Louis2012.
[43] J. Miura, Y. Maeda, H. Nakai, M. Zako, Multiscale analysis of stress distribution in teeth under applied forces, Dental Materials 25(1) (2009) 67-73.
[44] J.H. Kinney, S.J. Marshall, G.W. Marshall, The mechanical properties of human dentin: A critical review and re-evaluation of the dental literature, Critical Reviews in Oral Biology & Medicine 14(1) (2003) 13-29.
[45] P. Vallittu, Non-Metallic Biomaterials for Tooth Repair and Replacement, Cambridge woodhead2012.
[46] H.H.K. Xu, D.T. Smith, S. Jahanmir, E. Romberg, J.R. Kelly, V.P. Thompson, E.D. Rekow, Indentation damage and mechanical properties of human enamel and dentin, Journal of Dental Research 77(3) (1998) 472-480.
[47] J.L. Cuy, A.B. Mann, K.J. Livi, M.F. Teaford, T.P. Weihs, Nanoindentation mapping of the mechanical properties of human molar tooth enamel, Archives of Oral Biology 47(4) (2002) 281-291.
[48] E. Mahoney, A. Holt, M. Swain, N. Kilpatrick, The hardness and modulus of elasticity of primary molar teeth: an ultra-micro-indentation study, Journal of Dentistry 28(8) (2000) 589-594.
[49] J. Min, D.D. Arola, D.D. Yu, P. Yu, Q.Q. Zhang, H.Y. Yu, S.S. Gao, Comparison of human enamel and polymer-infiltrated-ceramic network material "ENAMIC" through micro- and nano-mechanical testing, Ceramics International 42(9) (2016) 10631-10637.
[50] Y. Zhang, M. Allahkarami, J.C. Hanan, Measuring residual stress in ceramic zirconia-porcelain dental crowns by nanoindentation, Journal of the Mechanical Behavior of Biomedical Materials 6 (2012) 120-127.
[51] T. Graber, U. Bjorn, B. Zachrisson, T. Büyükyilmaz, Orthodontics– current principles and technique, Mosby 2005.
[52] W. Brantley, T. Eliades, Orthodontic materials, scientific and clinical aspect, New York: Thieme Stuttgart2001.
[53] D. Bajaj, D.D. Arola, On the R-curve behavior of human tooth enamel, Biomaterials 30(23-24) (2009) 4037-46.
[54] B.R. Lawn, J.J.W. Lee, Analysis of fracture and deformation modes in teeth subjected to occlusal loading, Acta Biomaterialia 5(6) (2009) 2213-2221.